1.0 GHz Monolithic p-i-n MODFET Photoreceiver Using Molecular Beam Epitaxial Regrowth

Paul R. Berger, Niloy K. Dutta, Dexter A. Humphrey, Peter R. Smith, Shuenn-Jyi Wang, R.K. Montgomery, D. Sivco, and A. Y. Cho

Abstract—**A single-stage integrating front-end photoreceiver comprised of a p-i-n $In_{0.53}Ga_{0.47}As$ photodiode integrated with a selectively regrown pseudomorphic $In_{0.65}Ga_{0.35}As$ / $In_{0.52}Al_{0.48}As$ MODFET using MBE regrowth was investigated. Cutoff frequencies of the 1.0 μm regrown MODFET's were f_t = 24 GHz and f_{max} = 50 GHz. Transconductance of the regrown MODFET's were as high as 495 mS / mm with a current density (I_{ds}) of 250 mA / mm. The 3-dB bandwidth of the photoreceiver was measured to be 1 GHz. The bit rate sensitivity at 1 Gb / s was −29.6 dBm for BER 10^{-9} using 1.55 μm excitation. The single-stage amplifier exhibited up to 25 dB flatband gain of the photocurrent.**

INTRODUCTION

FURTHER developments in InP-based optoelectronic circuits (OEIC) are continually improving the performance level of front-end photoreceivers. The design of a photoreceiver can follow three approaches to growth which allows two devices of disimilar epilayers to be incorporated on the same wafer. The first is a straight forward integration which uses a single epitaxial growth where the epilayer consists of both structures on top of each other. Uchida *et al.* [1] employed such a scheme using a cascode amplifier and reported a sensitivity of −34.7 dBm at 622 Mb/s. Uchida *et al.* actually employed a p-i-n-JFET integration in which the same epilayer was utilized as the two devices, but Be implantation was necessary to create the p-i-n photodiode. Chandrasekhar *et al.* [2] employed the more traditional vertical integration with a p-i-n photodiode underneath a HBT. Using a transimpedance design, Chandrasekhar *et al.* demonstrated a bit rate sensitivity of −18.8 dBm at 5 Gb/s for a wafer grown by chemical beam epitaxy (CBE). A second growth alternative is to grow a single epitaxial growth sequence on a patterned substrate. Usually the transistor is grown first to reduce parasitics under the transistor. To fabricate the transistor, the overlaying photodiode is etched away atop the substrate mesas, using an etch-step layer. Chang *et al.* [3] employed a transimpedance design which exhibited a 3 GHz bandwidth using a MSM-HEMT integration grown by OMCVD. Yano *et al.* [4] used a p-i-n-HEMT design which achieved a sensitivity of −30.4 dBm at 1.2 Gb/s by OMVPE using an internal equalizer to improve sensitivity. The third growth approach is to grow the disimilar layer structures with two growths and pattern the wafer after the first growth with a dielectric mask. Selective area regrowth will result, and allows the final device integration to be planar and avoids any distributed capacitances created by one device vertically integrated with another. Nobuhara *et al.* [5] used this technique to integrate a p-i-n photodiode with a HEMT using MBE. It exhibited a sensitivity of −23.7 dBm at 2 Gb/s. Antreasyan *et al.* [6] used a p-i-n photodiode integrated with a MISFET using two VPE growths. They demonstrated receiver sensitivity of −25.4 dBm at 600 Mb/s using a single stage amplifier. Zebda *et al.* [7] used a p-i-n-MODFET integration with two succesive MBE growths and demonstrated a 6.5 GHz bandwidth with 0.25 μm gate lengths, but reported no sensitivity measurements. We are reporting on a simple single-stage integration front-end photoreceiver comprised of a p-i-n $In_{0.53}Ga_{0.47}As$ photodiode integrated with a selectively regrown pseudomorphic $In_{0.65}Ga_{0.35}As/In_{0.52}Al_{0.48}As$ 1.0 μm π-gate MODFET.

EXPERIMENTAL

The p-i-n photodiode is grown by MBE first. The p-i-n photodiode consisted of a superlattice (SL) buffer, a 0.4 μm n^+-$In_{0.52}Al_{0.48}As$ lower contact layer, a 0.75 μm i-$In_{0.53}Ga_{0.47}As$ active region with 300 Å i-$In_{0.52}Al_{0.48}As$ setback layers above and below to minimize impurity interdiffusion, a 0.4 μm p^+-$In_{0.52}Al_{0.48}As$ upper contact layer, and a 200 Å n^+-$In_{0.53}Ga_{0.47}As$ cap layer. A heterojunction photodiode reduces the dark current created by generation and recombination of carriers in the higher bandgap material, and the upper contact acts as an optical window. The epilayer is then coated with SiO_2 using plasma enhanced chemical vapor deposition (PECVD). The wafer is then patterned photolithographically and mesas are formed in the p-i-n material by chemically removing the surrounding material down to the InP substrate. The wafer is cleaned and reinserted into the MBE for regrowth of the MODFET. The MODFET structure is comprised of a SL buffer, a i-$In_{0.52}Al_{0.48}As$ buffer, a 400

Manuscript received March 25, 1992; revised May 7, 1992.
The authors are with AT & T Bell Laboratories, Murray Hill, NJ 07974.
IEEE Log Number 9201786.

1041-1135/92$03.00 © 1992 IEEE

Å i-$In_{0.53}Ga_{0.47}As$ layer, a 100 Å strained i-$In_{0.65}Ga_{0.35}As$ channel layer, a 50 Å i-$In_{0.52}Al_{0.48}As$ spacer layer, a 150 Å n^+-$In_{0.52}Al_{0.48}As$ donor layer (5×10^{18} cm^{-3}), a 400 Å i-$In_{0.52}Al_{0.48}As$ layer to reduce gate leakage, and a 200 Å n^+-$In_{0.53}Ga_{0.47}As$ cap layer. Polycrystalline material grows on top the SiO_2 mask, and single crystal material beside the p-i-n mesa. The wafer is again patterned and the polycrystalline material and SiO_2 is selectively removed by wet etching. The planar wafer is then processed conventionally to build the circuit. Isolated p-i-n photodiodes and MODFETs are included in the mask for diagnostic purposes. The MODFET's employ a π-gate configuration to reduce the gate resistance. The gates lengths are 1.0 μm using contact lithography and the gate widths are varied (2×40, 2×75, and 2×100 μm wide). A schematic of the p-i-n-MODFET photoreceiver circuit is shown in Fig. 1. Resistors composed of 600 Å Ti were used.

Results

The dc characteristics of the MODFET's were measured from isolated devices on the same processed wafer as the integrated circuits. The I–V characteristics of a regrown $2 \times (1.0 \times 100$ μm) π-gate MODFET are shown in Fig. 2(a). The extrinsic transconductance (g_m) of the as-grown MODFET's was as high as 546 mS/mm with current densities (I_{ds}) up to 317 mA/mm at $V_{ds} = 1.5$ V, while the regrown MODFETs had up to 495 mS/mm at current densities up to 250 mA/mm. Therefore, the regrown MODFET's only suffered a roughly 10% performance degradation due to regrowth. The transfer characteristics of the regrown MODFET shown in Fig. 2(a) are shown in Fig. 2(b). A summary of the dc values for various gates widths of both as-grown and regrown MODFET's are listed in Table I.

Device figures of merit, f_t and f_{max} were measured using a vector network analyzer and wide bandwidth coplanar waveguide probes. Measurements were made from 100 MHz to 40 GHz. The parasitic effects of the pads were removed by subtracting the Y parameters of the pads without a device from the Y parameters of the device and pads. Pads alone, and devices, were measured under the same conditions, and were located near each other. The devices were biased for maximum transconductance. As-grown MODFET's had cutoff frequencies as high as $f_t = 58$ GHz and $f_{max} = 67$ GHz. Regrown MODFET's had $f_t = 24$ GHz and $f_{max} = 51$ GHz. The cutoff frequencies, f_t and f_{max}, were obtained by extrapolating the curves at −6 dB/octave. Summaries of the cutoff frequencies and flatband gain (H_{21}) of the as-grown and regrown MODFET's are also included in Table I. The degraded microwave performance of the regrown MODFET's correlated with the increase in the output conductance (g_{gs}) from the equivalent circuit obtained from the measured S-parameters. The increased output conductance effectively creates an internal shunt which reduces the gain and thus lowers the cutoff frequencies. Lai *et al.* [8] studied regrown MODFET's and attributed the degradation to an increase in the density of slow traps in the InAlAs underneath the channel arising from impurities or defects out-diffusing from the regrown interface and riding with the growth front.

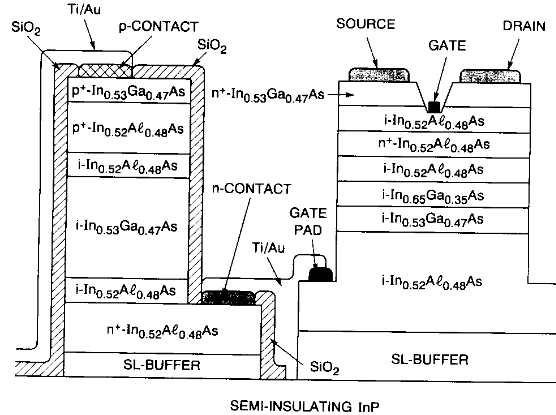

Fig. 1. Schematic of the p-i-n-MODFET circuit.

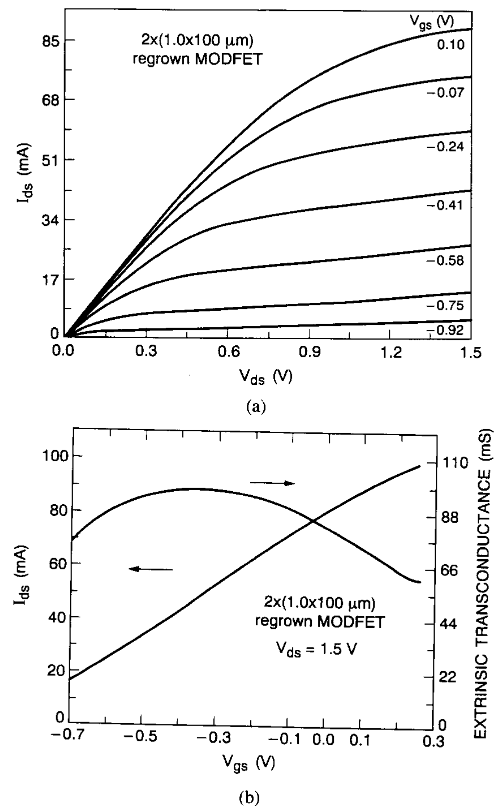

Fig. 2. (a) $I_{ds} - V_{ds}$ characteristics of a regrown $2 \times (1.0 \times 100$ μm) π-gate pseudomorphic $In_{0.65}Ga_{0.35}As/In_{0.52}Al_{0.48}As$ MODFET ($V_{g,start} = 0.1$ V, $V_{g,step} = -0.17$ V). (b) Transfer characteristics ($g_m - V_{gs}$ and $I_{ds} - V_{gs}$) of a regrown $2 \times (1.0 \times 100$ μm) π-gate pseudomorphic $In_{0.65}Ga_{0.35}As/In_{0.52}Al_{0.48}As$ MODFET.

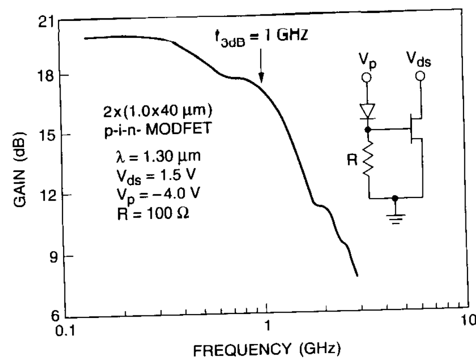

Fig. 3. Measured small signal frequency response of the monolithic p-i-n-MODFET circuit using a pseudomorphic $2 \times (1.0 \times 40\ \mu m)$ $In_{0.65}Ga_{0.35}As/In_{0.52}Al_{0.48}As$ MODFET ($V_{ds} = 1.5$ V and $V_p = -4.0$ V).

The dc characteristics were measured of the isolated p-i-n photodiodes which were subjected to regrowth conditions, and they exhibited leakage current which ranged from 30 nA to 300 nA at −5 V and breakdown voltages of 18–20 V. The photodiodes after experiencing the temperature cycling of regrowth had a series resistance of ~14 Ω. The $30 \times 40\ \mu m^2$ p-i-n photodiode has a junction capacitance of 0.19 pF.

The responsivity of the photodiodes was measured using a 1.55 µm InGaAsP laser diode. The collected photocurrent was measured and compared to the response of a calibrated large area Ge photoconductor. The laser light was focused down onto the $30 \times 40\ \mu m^2$ photodiode. The spot size was slightly larger than the diode size. The measured responsivity is ≥0.41 A/W and estimates of the actual responsivity due to the uncompensated large spot size range up to ~0.55–0.60 A/W.

The bandwidth of the circuit was measured using a network analyzer with a lightwave test set which included a 1.3 µm laser source, the output of which could be modulated from 130 MHz–20 GHz. The wafers were probed on-chip with a microwave probe station and light was focused onto the photodiode using a fiber-optic probe. The circuit, shown in Fig. 3, was biased with $V_{ds} = 1.5$ V and the photodiode reverse biased at $V_p = -4.0$ V. The 3-dB bandwidth ranged up to 1 GHz, as shown in Fig. 3. No external output buffer or equalizer was utilized. The p-i-n photodiodes were measured in a similar manner and exhibited a 3-dB bandwidth of up to 1.7 GHz. The gain for the receiver circuits was measured to be 20.0, 22.3 and 24.8 dB over the p-i-n photodiode for the $2 \times (1.0 \times 40\ \mu m)$, $2 \times (1.0 \times 75\ \mu m)$ and $2 \times (1.0 \times 100\ \mu m)$ MODFET's, respectively. The gain was calibrated with isolated p-i-n photodiodes on the same wafer which were similarly measured.

The receiver sensitivity was measured at 1 Gb/s using a 1.55 µm PRBS = $2^{15} - 1$ NRZ signal. The sensitivity as a function of the average power ($\bar{P}$) is plotted and shown in Fig. 4. The receiver sensitivity was measured to be −29.6 dBm for a $2 \times (1.0 \times 40\ \mu m)$ MODFET at a BER of 10^{-9}. Fig. 5 shows the eye pattern for the measured device in Fig. 4. A clear open eye is evident.

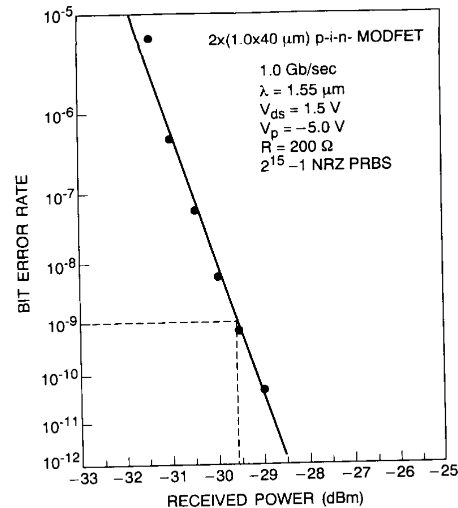

Fig. 4. Sensitivity of the monolithic p-i-n-MODFET circuit using a pseudomorphic $2 \times (1.0 \times 40\ \mu m)$ $In_{0.65}Ga_{0.35}As/In_{0.52}Al_{0.48}As$ MODFET ($V_{ds} = 1.5$ V and $V_p = -5.0$ V).

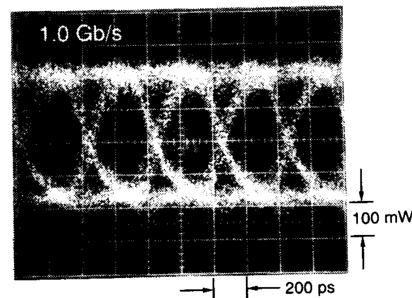

Fig. 5. Eye diagram of the monolithic p-i-n-MODFET circuit using a pseudomorphic $2 \times (1.0 \times 40\ \mu m)$ $In_{0.65}Ga_{0.35}As/In_{0.52}Al_{0.48}As$ MODFET ($V_{ds} = 1.5$ Vand $V_p = -5.0$ V).

Summary

A p-i-n-MODFET photoreceiover was fabricated and tested using MBE selective area regrowth. Cutoff frequencies (f_T and f_{max}) of 58 and 67 GHz were measured for the as-grown and regrown MODFET's, and 24 and 51 GHz for the regrown MODFET's, respectively. The sensitivity of the p-i-n-MODFET photoreceiver at 1 Gb/s was −29.6 dBm which is more than 4 dB greater sensitivity than other single-stage OEIC photoreceivers and within 1–2 dB of the best multiple-stage OEIC photoreceivers.

Acknowledgment

We are grateful to Y. K. Chen who provided help with the bandwidth measurements.

TABLE I
SUMMARY OF DC AND MICROWAVE MEASUREMENTS OF AS-GROWN AND REGROWN π-GATE PSEUDOMORPHIC $In_{0.65}Ga_{0.35}As/In_{0.52}Al_{0.48}As$ MODFET'S WITH VARYING GATE WIDTHS

Parameter	As-Grown MODFET			Regrown MODFET		
	2×40 μm	2×75 μm	2×100 μm	2×40 μm	2×75 μm	2×10 μm
g_m (mS/mm)	546	540	545	479	495	487
I_{ds} (mA/mm)	267	303	317	235	250	229
H_{21} (dB)*	47.0	55.0	50.0	31.1	33.9	33.9
f_t (GHz)	46.4	58.4	55.3	23.1	22.6	24.3
f_{max} (GHz)	67.3	51.7	42.2	50.5	40.3	40.2

* Flatband gain.

REFERENCES

[1] N. Uchida, Y. Akahori, M. Ikeda, A. Kohzen, J. Yoshida, T. Kokubun, and K. Suto, "A 622 MB/s high-sensitivity monolithic InGaAs-InP pin-FET receiver OEIC employing a cascode preamplifier," *IEEE Photon. Technol. Lett.*, vol. 3, pp. 540–542, 1991.

[2] S. Chandrasekhar, A. H. Gnauck, W. T. Tsang, F. S. Choa, and G. J. Qua, "A monolithic 5 Gb/p p-i-n/HBT integrated photoreceiver circuit realized from chemical beam epitaxial material," *IEEE Photon. Technol. Lett.*, vol. 3, pp. 823–825, 1991.

[3] G.-K. Chang, W. P. Hong, J. L. Gimlett, R. Bhat, C. K. Nguyen, G. Sasaki, and J. C. Young, "A 3 GHz transimpedance OEIC receiver for 1.3–1.55 μm fiber-optic systems," *IEEE Photon. Technol. Lett.*, vol. 2, pp. 197–199, 1990.

[4] H. Yano, K. Aga, H. Kamei, G. Sasaki, and H. Hayashi, "Low-noise current optoelectronic integrated receiver with internal equalizer for gigabit-per-second long-wavelength optical communications," *J. Lightwave. Technol.*, vol. 8, pp. 1328–1333, 1990.

[5] H. Nobuhara, H. Hamaguchi, T. Fuji, O. Aoki, M. Makiuchi, and O. Wada, "Monolithic pinHEMT receiver for long wavelength optical communications," *Elect. Lett.*, vol. 24, pp. 1246–1248, 1988.

[6] A. Antreasyan, P. A. Garbinski, V. D. Mattera, Jr., H. Temkin, N. A. Olsson, and J. Flipe, "Monolithically integrated InGaAs-P-I-N InP-MISFET pinFET grown by chloride vapor phase epitaxy," *IEEE Photon. Technol. Lett.*, vol. 1, pp. 123–125, 1989.

[7] Y. Zebda, R. Lai, P. Bhattacharya, D. Pavlidis, P. R. Berger, and T. L. Brock, "Monolithically integrated InP-based front-end photoreceivers," *IEEE Trans. Elect. Dev.*, vol. 38, pp. 1324–1333, 1991.

[8] R. Lai and P. K. Bhattachraya, "Performance characteristics of $In_{0.53}Ga_{0.47}As/In_{0.52}Al_{0.48}As$ modulation-doped field-effect transistors realized by two-step epitaxy: Effects of molecular beam epitaxial regrowth," *J. Appl. Phys.*, vol. 67, pp. 4345–4348, 1990.

Optical Monitoring for Plasma-Etching Depth Process

Shizhuo Yin, Francis T. S. Yu, *Fellow, IEEE,* and Shudong Wu

***Abstract*—In this letter, a novel technique for monitoring the opaque thin-film etching depth during the plasma-etching process is presented. The feature of this technique is that a small Laminar grating is overlaid on the empty region of the wafer along with the etching pattern. By coherent illumination, a reflected intensity distribution from the Laminar grating for different orders of diffraction can be obtained. Since the etching depth and the diffraction distribution are related, by analyzing the intensity profiles due to Laminar depth grating, the etching depth of the specimen can be measured. We have shown that the accuracy of this measurement can be as high as 100 Å.**

Manuscript received April 16, 1992; revised May 20, 1992. This work was supported by the Applied Research Laboratory at the Pennsylvania State University.

S. Yin and F. T. S. Yu are with the Department of Electrical and Computer Engineering, The Pennsylvania State University, University Park, PA 16802.

S. Wu is with the Physical Opt. Co., Torrance, CA 90501.

IEEE Log Number 9202021.

PLASMA etching is commonly used as a cheaper alternative to wet solvent resist stripping for integrated circuit manufacture [1]. The impetus of this change comes from the inherent merits of plasma etchings. First, the plasma etching is a dry process, which is simple and convenient to operate. Second, the plasma etching is an anisotropic process, by which a higher resolution can be achieved.

One of the most important aspects of the plasma etching is that the etching depth can be monitored during the process. There are two commonly used methods for monitoring the plasma etching depth; one uses the laser interferometric technique [2], which is based on the interference fringes obtained from the front surface and the underlying interface of the thin transparency. This method is simple and practical, but it is only suitable for the transparent films. The other method is using ellipsometry

1041-1135/92$03.00 © 1992 IEEE